Supporting Information

Bencherif et al. 10.1073/pnas.1211516109

SI Materials and Methods

Hydrogel Characterization. Structural analysis of the macroporous gels was performed using a LEO 982 scanning electron microscope (SEM) (LEO Electron Microscopy). To prepare the samples, cryogels in the frozen state following cryogelation were lyophilized and sectioned for observation. The distribution of cells within the scaffolds was also imaged using SEM. Cell-seeded cryogels were washed with PBS, and cells were fixed in 2.5% glutaraldehyde. After the incubation period, scaffolds were rinsed in PBS and dehydrated by gradually increasing ethanol followed by drying in vacuum desiccators. The dried samples were then coated with gold and analyzed by SEM. The average size of pores in cryogels was calculated by averaging the diameters of the pores in the gels observed by SEM.

Micro-computed tomography (micro-CT) was used to analyze the 3D architecture and structural homogeneity of the porous material using micro-CT equipment (HMXST225, X-Tek; Nikon Metrology NV) with associated software (CT Pro software).

The pore connectivity was further evaluated using a water-wicking technique in which the interconnected porosity was calculated as the interconnected void volume over the total volume. To determine total volume, gels were soaked in water for 1 h and weighed. A Kimwipe was then used to wick away water within interconnected pores, and the gels were weighed once again. The interconnected void volume was calculated as the volume of water wicked from the gels.

Young's modulus was determined using an Instron testing system (Instron 3342). Cylindrical hydrogels (8-mm diameter, 5-mm height) were deformed (at constant volume) between two parallel plates with a strain rate of 20% per minute. Engineering stresses and strains were recorded. The gel cylinders were kept hydrated in PBS solution (pH 7.4) throughout the tests.

The swelling ratio was determined using a conventional gravimetric procedure. To investigate the swelling ratio of each sample, cryogels and conventional cylindrical gels were prepared and immersed in PBS. The equilibrium mass swelling ratio (Q_M) was calculated by the following equation:

$$Q_M(\%) = [m_s/m_d \times 100],$$

where m_s and m_d were fully swollen gel and dried gel weights, respectively. The swelling data were corrected by subtracting the soluble fraction of salt in PBS from the gel.

Preparation of BSA-Containing Cryogels. BSA labeled with rhodamine was suspended in a liquid precursor solution before cryopolymerization. Briefly, 10 mg [1% (wt/vol)] of methacrylated (MA)-alginate in deionized water was mixed with rhodamine-labeled BSA [Rhod-BSA or Rhod-BSA-MA, 0.3% (wt/vol)], TEMED [0.5% (wt/vol)], and APS [0.25% (wt/vol)]. Rhod-BSA is physically entrapped within the polymer network, whereas Rhod-BSA-MA is covalently bound to the cryogel due to reactive methacrylate residues. The mixture was immediately poured into a precooled Teflon mold and frozen at −20 °C. After the fabrication process, the cryogels were thawed and washed to remove free BSA. Thereafter, the solution from the washing step was collected and used to determine the concentration of free BSA after cryogelation, thus providing the concentration of nonencapsulated protein. Fluorescence spectroscopy (Synergy HT; BioTek) was used to detect the fluorescence of rhodamine-labeled BSA. The absorbance value of each sample was read at 490 nm with a microplate reader. Wells containing deionized water were used as blank control and background. The encapsulation efficiency of the fluorescent protein was determined by comparing the absorbance of free BSA and the initial concentration of BSA.

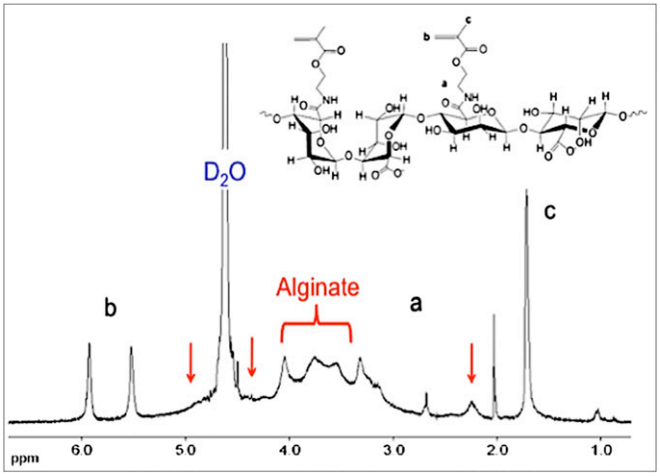

Fig. S1. ^{1}H NMR of MA-alginate demonstrating its characteristic vinylic peaks (δ5.3–5.8 ppm). Deuterated water (D_2O) was used as solvent, and the polymer concentration was 1% (wt/vol). The efficiency of alginate methacrylation was calculated based on the ratio of the integrals for alginate protons to the methylene protons of methacrylate. MA-alginate macromonomer was found to have approximately a degree of methacrylation (DM) of 50%.

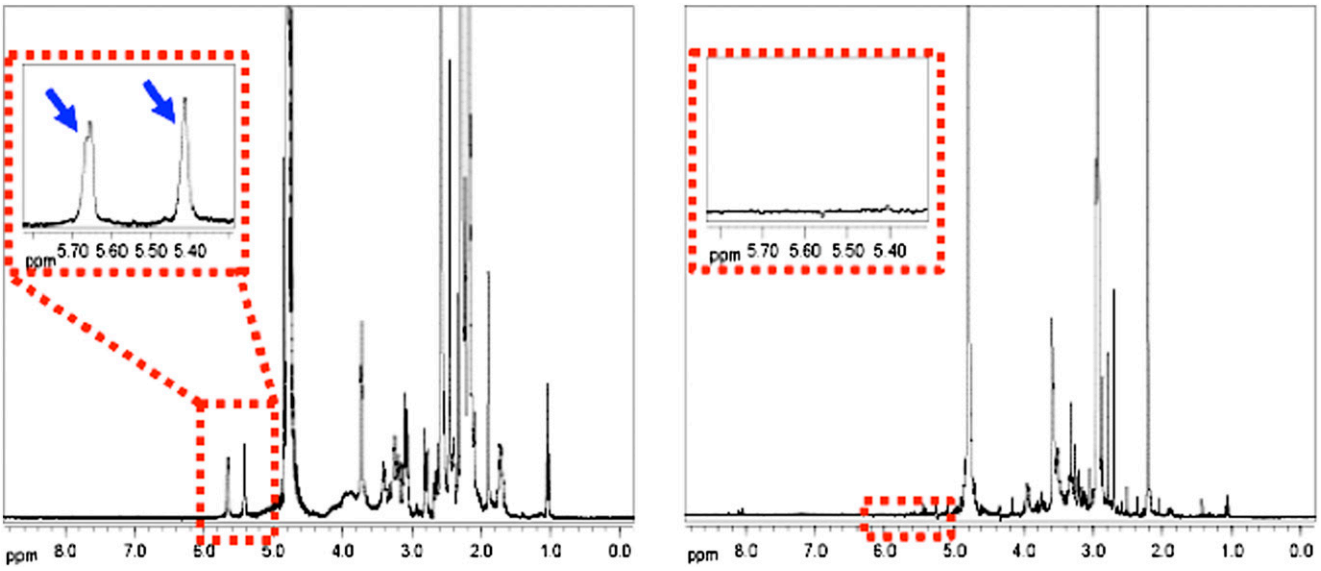

Fig. S2. ^{1}H NMR of un–cross-linked (*Left*) and cryopolymerized (*Right*) 1% (wt/vol) MA-alginate in D_2O. Cryogelation is induced directly in an NMR tube. One milliliter of macromonomer solution containing the initiator system was transferred into the NMR tube before cryogenic treatment at −20 °C for 17 h. The vinylic peaks (between δ5.3 and 5.8 ppm) disappeared after cross-linking. The conversion was evaluated by comparing the relative peaks of un–cross-linked and cross-linked methylene protons.

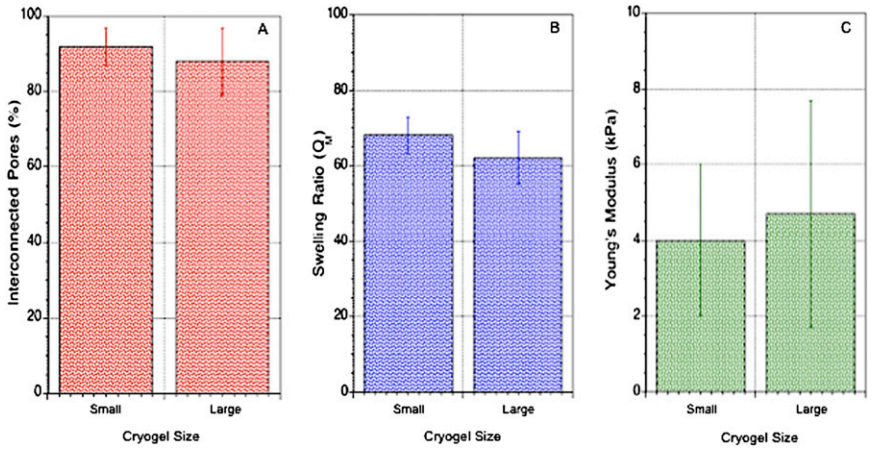

Fig. S3. Effect of gel size on the physical properties of alginate-based cryogels. Evaluation of pore connectivity (*A*), weight swelling ratio (*B*), and mechanical properties (Young's modulus) (*C*) of cylindrical cryogels prepared with two different sizes; small (8-mm diameter × 5-mm thickness) and large (12-mm diameter × 5-mm thickness). Values in *A*–*C* represent mean and SD (n = 3).

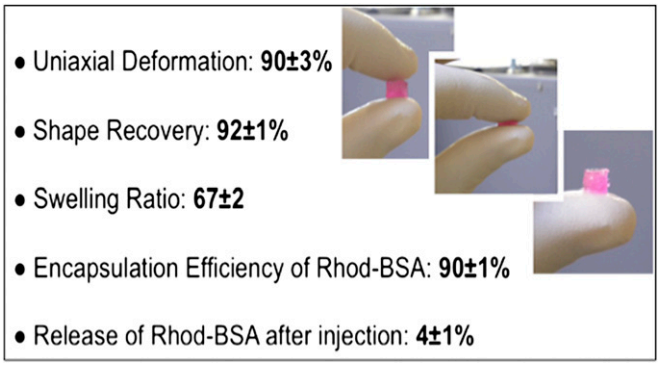

Fig. S4. Properties of 1% (wt/vol) alginate cryogels encapsulating 0.3% (wt/vol) Rhod-BSA. Uniaxial deformation and swelling measurements were performed as described in *SI Materials and Methods*. The shape recovery measurements were calculated based on the ratio of the weights of reswollen cryogel and initial fully swollen cryogel. Encapsulation efficiency [$E_E = 100 \times (A_i - A_r)/A_i$] of rhodamine-labeled BSA was calculated by measuring the spectroscopic absorbance at 490 nm of initial quantity of BSA used in encapsulation (A_i) and recovered free BSA (A_r) after cryopolymerization. Release of BSA [$R_{BSA} = 100 \times (R_b - R_a)/R_b$] during injection was calculated by measuring the spectroscopic absorbance at 490 nm of BSA-loaded cryogels before (R_b) and after (R_a) syringe injection through a fine needle (1 cc, 16G). All experiments were performed in triplicate, and mean and SD are reported. *Insets* show photographs of cylindrical MA-alginate cryogels: (*Left*) equilibrium swollen cryogel, (*Center*) cryogel compressed between fingers, and (*Right*) reswollen cryogel upon removal of force.

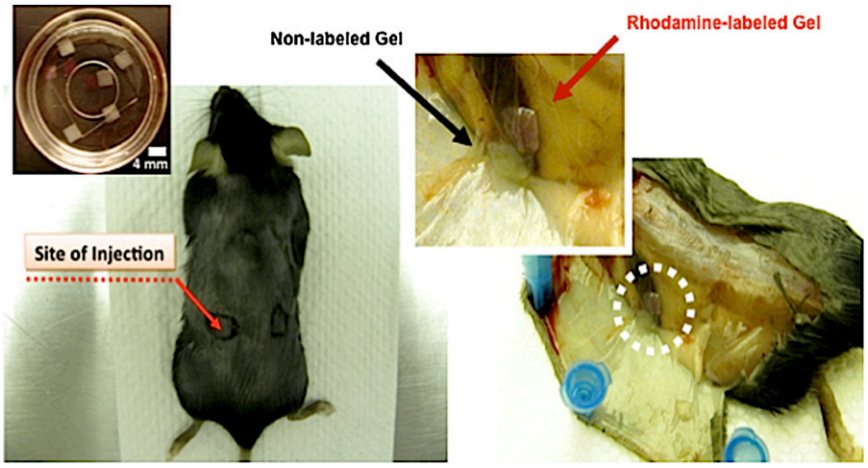

Fig. S5. The cryogels were successfully injected in vivo, recovered their original shapes, and remained localized at the point of introduction. *Inset* shows a zoom-in view of injected cryogels with geometric restoration.

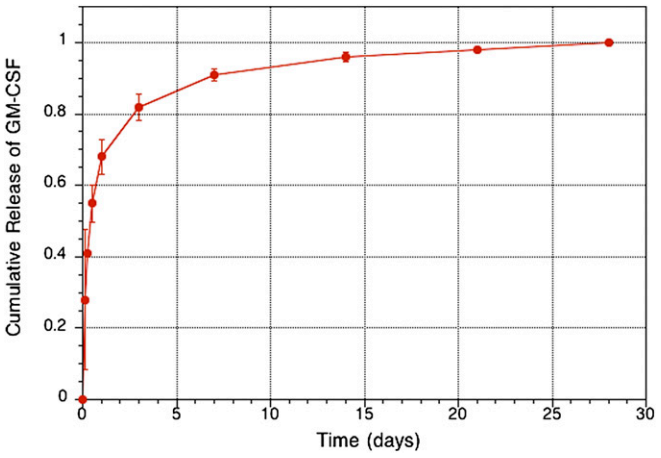

Fig. S6. Controlled release of recombinant murine granulocyte–macrophage colony-stimulating factor (GM-CSF) (PeproTech) from 1% (wt/vol) MA-alginate cryogels. Similarly to BSA, GM-CSF (1.8 μg/cryogel) was physically entrapped in square-shaped cryogels (4 × 4 × 1 mm) during the cryopolymerization process (encapsulation efficiency, 89%). The cryogels ($n = 5$) were transferred into a 12-well plate. Each cryogel was suspended in 1 mL of PBS containing 1% BSA as a carrier protein and incubated at 37 °C with gentle shaking (80 rpm). GM-CSF release in the supernatant was detected by ELISA (Invitrogen).

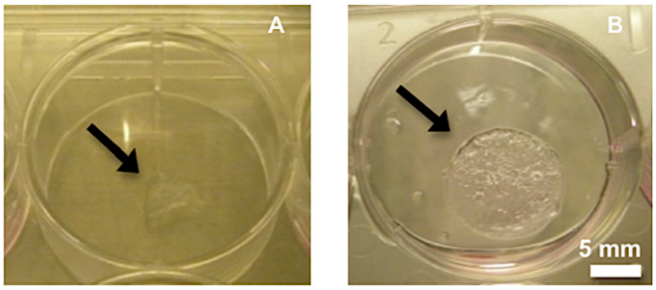

Fig. S7. Partially collapsed gels reswelled instantaneously in cell/media suspension. Cells enter and get entrapped inside the cryogels during rapid water absorption while the gels return to their equilibrium shapes and volumes as depicted in the photographs before (*A*) and after (*B*) gel seeding and restoration, as indicated by the arrows.

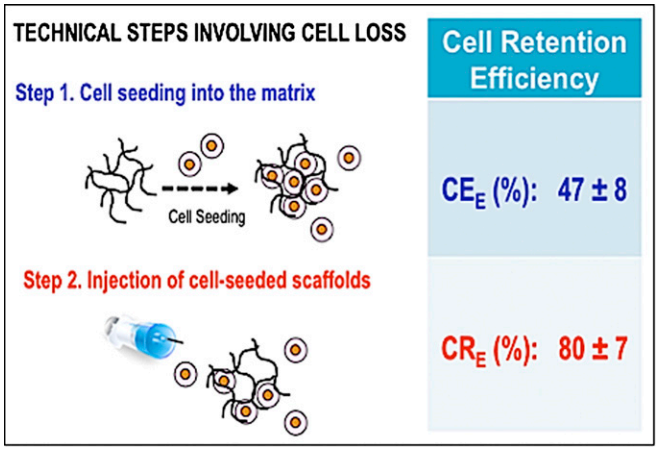

Fig. S8. Cell retention efficiency after cell seeding and injection of cell-seeded scaffolds. Cell entrapment efficiency during seeding ($CE_E = (C_{BS}-R_{C1})/C_{BS}$) was determined by counting the initial number of cells before seeding (C_{BS}) and comparing to recovered free cells (R_{C1}) after seeding (step 1). Cell retention efficiency after injection ($CR_E = (E_C-R_{C2})/E_C$) was determined by counting the initial number of encapsulated cells ($E_C = C_{BS}-R_{C1}$) and recovered free cells (R_{C2}) after injection (step 2). Note that before scaffold injection, the scaffolds were incubated for 6 h to allow cell adhesion to the matrix. All experiments were performed in triplicate and mean and SD are reported.

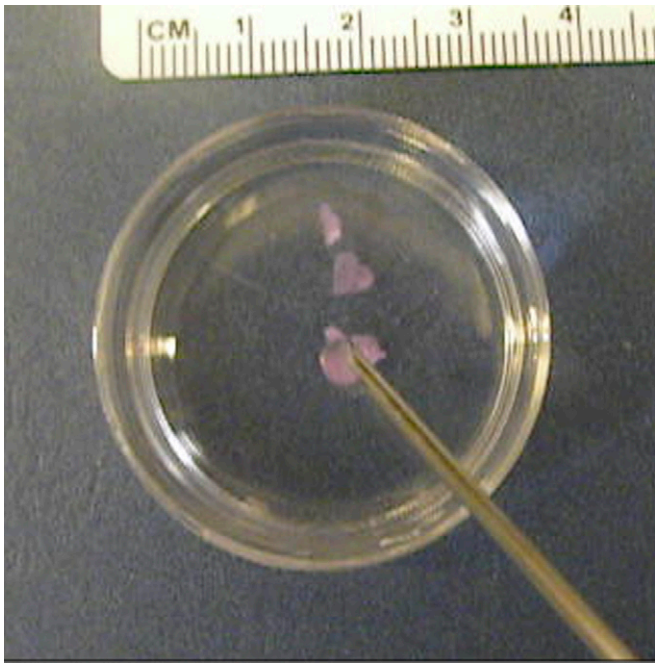

Movie S1. Shape-memory properties of geometric cryogels syringe injected via a 16-gauge needle.

Movie S1

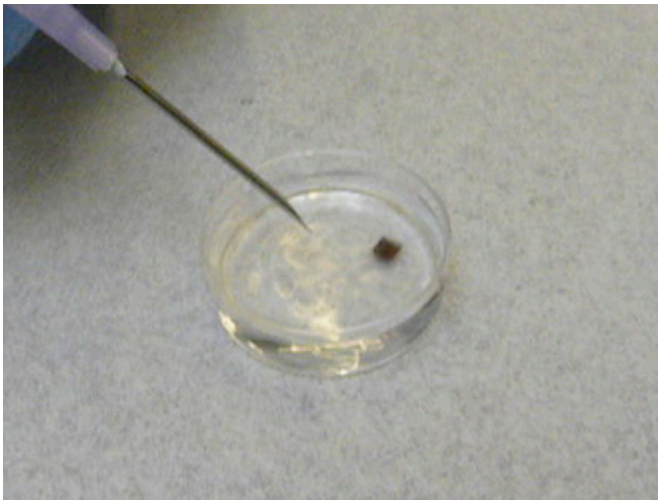

Movie S2. Rapid shape recovery of a square-shape cryogel after syringe injection.

Movie S2

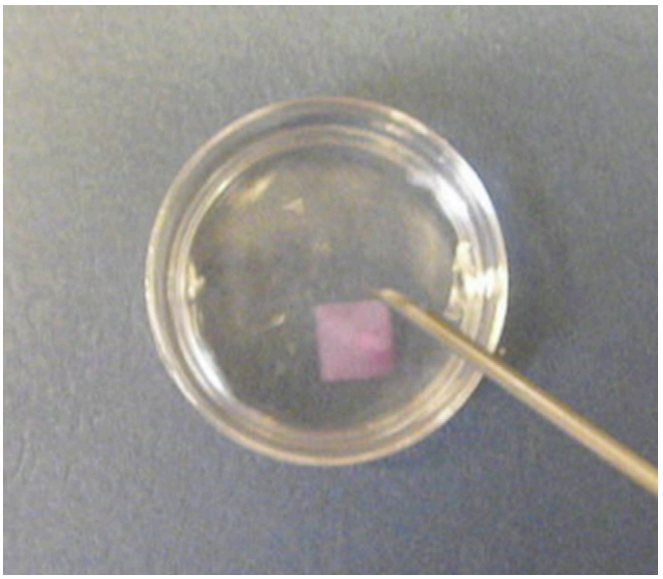

Movie S3. Successful syringe injection of a large square-shape (8 × 8 × 1 mm) preformed cryogel.

Movie S3

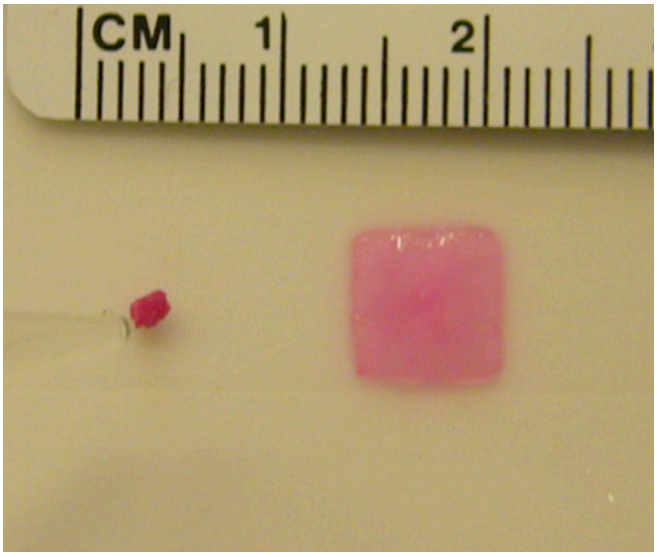

Movie S4. Collapsed cryogel regains its original memorized shape, size, and volume upon hydration.

Movie S4